Article

Advanced Science, Engineering and Medicine
Vol. 6, 1–8, 2014
www.aspbs.com/asem

Synthesis and Characterization of Colloidal TiO_2 Nanoparticles: Through Titanium Chloride Rich Solutions

Narendra Kumar Agrawal[1,*], Mangej Singh[2], Y. K. Vijay[2], and K. C. Swami[1]

[1] *Department of Physics, Malaviya National Institute of Technology, Jaipur 302017, India*
[2] *Department of Physics, University of Rajasthan, Jaipur 302055, India*

Nanoparticles of well-defined shape, controlled size having pure and clean surface are ideal model systems to investigate surface/interfacial reactions. The synthesis and characterization of colloidal TiO_2 nanoparticles having particles surface free from organic capping agents under well controlled experimental conditions are reported. The TiO_2 nanoparticles were synthesized, using two different approaches; one through aqueous hydrolysis of $TiCl_4$ and another trough basic oxidization of $TiCl_3$ where stable dispersions of TiO_2 nanoparticles of 5–10 and 15–20 nm were obtained respectively. The aqueous hydrolysis of $TiCl_4$ predominantly resulted into brookite phase while the basic oxidization of $TiCl_3$ yielded anatase phase TiO_2 nanoparticles. The TiO_2 nanoparticles were also tested for inactivation of *Escherichia coli* bacteria under fluorescent lamp for water purification.

Keywords: TiO_2 Nanoparticles, Anatase Phase, Brookite Phase, Particle Size Distribution, X-Ray Diffraction, Capping Agents.

1. INTRODUCTION

Photo-cleavage of water for producing H_2 and O_2 can be catalyzed using TiO_2. This discovery makes interests in utilizing TiO_2 in a wide range of applications such as photo-catalysis, water purification systems and solar cells.[1–3] Properties of TiO_2 nanoparticles can be enhance by reducing particle size below 20 nm. While narrow size particle distribution in suspension form is an efficient and reliable tool for greatly enhance efficiency, reactivity and compatibility of TiO_2 nanoparticles due to change in curvature of nanoparticle surface and creating a huge number of under-coordinated surface atoms leading to substantially more reactive surface sites especially when free from organics capping agents.[4–6]

The TiO_2 nanoparticles shows many size dependent properties and applications like: long-term stability, nontoxicity, low resistance, discoloration under UV light,[7] filler for coating on plastics and rubbers resultant nanocomposites,[8] improved performance in UV-shielding, dynamic fracture toughness, flame retardant, optical transparency,[9] scratch resistance, chemical resistance,[10] barrier properties,[11] dye-sensitized solar cells applications,[11] gas sensor,[12] nanomedicine,[13] cosmetic,[14] photo-electrochemical activity,[15] solar energy conversion,[16] photo catalysis,[17] mycobacterium activity,[18] UV detectors and ultrasonic sensors.[19] Environmental compatibility, non-toxicity and low price are some typical advantages of TiO_2. TiO_2 also has strong negative effect on the thermal stability of PVDF/PMMA because of its catalytic decomposition character.

TiO_2 nanoparticles can be synthesized of different size and shape using sol–gel, physical and hydrothermal methods.[20–23] But as reliable surface and interfacial properties such as surface charge densities and size dependent reactivity can be obtained for nano particles below 20 nm having clean surfaces, i.e., without stabilizing organic compounds and all of above methods based on reactions containing organic compounds, which are difficult to remove from the particle surfaces. It requires a method of synthesis in which nanoparticles below 20 nm with narrow particle size distributions and surface free from organic compounds can be synthesized. Organic capping agents free TiO_2 nanoparticles can be synthesized if chlorides of Ti ($TiCl_4$ and $TiCl_3$) will be used as a precursor and undergo aqueous hydrolysis and basic oxidization respectively. TiO_2 nanoparticles synthesized in chloride rich solution can have all three crystalline phase rutile, anatase and brookite but rutile and brookite found as major crystalline having different sizes and wide distribution.[24–25] Particles below 20 nm size having particular phase with narrow

*Author to whom correspondence should be addressed.

particle size distribution can be synthesized by using above precursors, under highly controlled experimental conduction i.e., constant PH (≈ 2), synthesis at constant temperature (0 °C), concentration of Ti precursor, constant stirring rate and other constant experimental conditions.

In present study detailed investigation is performed for synthesis of TiO_2 nanoparticles (< 20 nm) using different precursor of Ti ($TiCl_4$ and $TiCl_3$) under controlled aqueous hydrolysis and basic oxidization respectively. With careful optimization of reaction time, PH, synthesis temperature and concentration of Ti precursor. Stable and narrow dispersed TiO_2 nanoparticles are obtained with aqueous hydrolysis of $TiCl_4$ and basic oxidization of $TiCl_3$. The Phase, shape, size and particle size distributions of the TiO_2 particles are determined by X-ray diffraction (XRD) and transmission electron microscopy (TEM). TEM can give information of size distributions of particles and crystalline phase present in the colloidal solution. In such an analysis fraction of particles, usually few hundred, can be mapped for particle size determination and crystalline phase identification. These nanoparticles also characterized by Scanning electron microscope for morphology and EDXA for purity and chemical analysis of TiO_2 PNs. Optical properties are characterized by UV-Vis and PL spectrometer. The TiO_2 nanoparticles are also tested for inactivation of Escherichia coli bacteria under fluorescent lamp. To best of our knowledge this is the first time $TiCl_4$ has been used for synthesis of brookite phase nanoparticles of size range of 5–10 nm and $TiCl_3$ has been used for synthesis of anatase phase nanoparticles of size range 15–20 nm.

2. EXPERIMENTAL DETAILS

2.1. Material Synthesis

The TiO_2 nanoparticles are synthesized under controlled aqueous hydrolysis and basic oxidization of $TiCl_4$ and $TiCl_3$ respectively. To obtain small and narrow particle size distributions of TiO_2 nanoparticles, all optimized parameter like reaction time, PH, synthesis temperature, concentration of Ti precursor and other experimental condition were kept constant. The $TiCl_4$ ($TiCl_3$) [each 99.5% pure] was cooled at -20 °C in deep freezer, then 5 ml of this solution was taken into a caped stopping funnel and added drop wise into 250 mL of de-ionized Milli-Q water (250 ml, 25% NH_4OH solution) at reaction temperature of 0 ± 0.2 °C, under vigorous stirring. The synthesis was done using a 1:50 $\{TiCl_4(TiCl_3):H_2O(NH_4OH)\}$ volume ratio with a resulting TiO_2 concentration of ≈ 14.5 gL^{-1}. If not controlled hydrolysis of $TiCl_4$ occurs at very low PH, while basic oxidization of $TiCl_3$ was initially at high PH but as soon few ml (1–2 ml) solution of $TiCl_3$ mixed into NH_4OH PH of solution drops rapidly, due to formation of Cl^- ions and HCl vapors/fumes. This high Cl^- ions concentration in reaction mixture are responsible to aggregation of TiO_2 nanoparticles and formation of large particles. So to avoid aggregation of particles PH of the solution was maintained at 2 using PH meter. This can be achieved by slow mixing rate (3 ml/hrs) of $TiCl_4/TiCl_3$ into water/NH_4OH, so that excess HCl gas can evacuated and PH of the solution remain constant at 2, here it must be noted that caped stopping funnel containing $TiCl_4/TiCl_3$ is cooled below 0 °C using salt added ice bath so that vaporization of $TiCl_4/TiCl_3$ can be minimized. These reaction mixtures were undergo vigorous stirring for 24 hrs on magnetic stirrer at 0 °C, for complete removal of HCl gas and to obtained white uniformly dispersed TiO_2 nanoparticle suspension. TiO_2 nanoparticles of different sizes can be obtain by varying reaction temperature.[5] Hence temperature of the reaction solution was precisely controlled using a temperature control unit.

2.2. Characterization

2.2.1. X-Ray Diffraction

The crystalline structure of synthesized TiO_2 were recorded by X'Pert Pro X-ray diffractometer (PAN alytical BV, The Netherlands) operated at a voltage of 45 kV and current of 40 mA with Cu k(α) radiation of wavelength 1.54059 Å, at grazing angle of powder X-ray diffraction. The scanning was done in the region of 2θ from 22° to 68° at 0.030 Å per step and the time step as 5 s. Sample powder for XRD is prepared, by vacuum drying of synthesized TiO_2 dispersion obtained from different precursor of Ti at 10^{-3} mbar for 5 hrs continuous pumping. These dried TiO_2 samples were grind to fine powder. Crystalline size is determined using Scherrer's formula.[26] Crystalline phases are determined by using Powder-X software and phase composition is calculated using Gaussian fit analysis.[27] Reference diffraction data from JCPDS files for anatase (No. 21-1272) and brookite (No. 29–1360) were used.

2.2.2. Transmission Electron Microscopy

The particle size and morphology of TiO_2 nanoparticles is determined by transmission electron microscopy (TEM). The imaging is performed using a Technika TEM instrument operating at 200 kV. The TiO_2 Nanoparticles obtained from different precursor of Ti were vacuum dried at 10^{-3} mbar for 5 hrs continuous pumping and then dispersed solution of these particles are prepared in acetone by ultra-sonication. A drop of this stable particle dispersion is kept and dried on a carbon coated copper (3 mm diameter) TEM grid.

2.2.3. Scanning Electron Microscopy and EDAX Measurements

The particle size and morphology of TiO_2 nanoparticles is also determined by SEM, while purity and chemical analysis was done with EDAX. SEM analysis was done using scanning electron microscope (Carl ZEISS EVOR-18) operated at 15 kV. Sample for SEM and EDAX

analysis are prepared on a Si substrate. Few drops of each stable particle dispersion of TiO_2 nanoparticles obtained from different precursor of Ti are loaded on different Si substrate and allowed to dry at room temperature in a closed chamber. These samples were used for SEM and EDAX analysis. EDAX measurement of TiO_2 nanoparticles were performed on same SEM instrument equipped with an Oxford instrument nano analysis X-act EDAX attachment.

2.2.4. UV-Visible and Photoluminescence (PL) Spectroscopy

UV-Visible spectral analysis is done using a double beam spectrophotometer (UV-1800 ENG240V SOFT SHIMADZU) and PL emission spectra of synthesized TiO_2 nanoparticles are recorded by (RF5301 PL SHIMADZU) Spectra fluorimeter using a four side polished quartz cuvette of path length 10 mm. Few drops of synthesized stable particle dispersion of TiO_2 nanoparticles were diluted with Milli-Q water and directly used for UV-Vis and PL analysis.

2.2.5. Photo-Catalytic Study: Inactivation of Escherichia Coli Bacteria

TiO_2 shows photo catalyst activity, including successful killing of cancer cells, bacteria, viruses, fungi and algae under UV illumination and toxic ingredient of bacteria can also be decomposed.[28–31] *E. coli* cells can be killed completely after 1 h of UV illumination on TiO_2 films but if TiO_2 nanopowder is used in UV light, only 0.25 g/L TiO_2 is needed to inactivate *E. coli* cells.[32] Hence we have tested survival of *E. coli* in TiO_2 nanoparticles suspension synthesized by different precursors of Ti in the presence of UV light.

Standard *E. coli* inoculums are prepared by the method as described by Ainon et al.[33] 10 ml solutions having 0.1, 0.25 and 1.0 g/L of TiO_2 nanoparticles in normal saline is prepared, using each type (prepared by $TiCl_4$ and $TiCl_3$) of nanoparticles prior to photo catalytic reaction and kept in the dark. 10% of fresh standard inoculums of *E. coli* ($\approx$ 115 cfu/mL) are inoculated in 100 mL sterilized normal saline. Then each 10 ml TiO_2 nanoparticles suspension is mixed with *E. coli* cells using magnetic stirrer and bead and illuminated with UV light at 25 cm from the surface of medium. Control is prepared using an *E. coli* ($\approx$ 115 cfu/mL) suspension without TiO_2. Few drops of *E. coli* –TiO_2 suspension sample are removed at each 1 h interval for 8 hours. After serial dilutions of these samples in normal saline, concentration of *E. coli* is enumerated using spreading plate method on nutrient agar (NA). These plates are incubated at 37 °C for 12 hrs and the colonies were counted using colony counter. Survival percentage of E-coli is determined by $[(X-Y)*100/X]$ where X and Y are number of colony (cfu/mL) before and after treatment respectively.

3. RESULTS AND DISCUSSION

X ray diffraction pattern of TiO_2 samples obtained using different precursor of Ti are shown in Figure 1. XRD measurements were performed after five days of synthesis, with crushed, vacuum dried TiO_2 powder. Strongest peak for TiO_2 Nanoparticles synthesized by $TiCl_4$ was observed B (2 2 1) at reflection $2\Theta = 25.4°$. Other crystalline planes comes at B (1 2 1), A (0 0 4), B (2 0 1), A (2 0 0), A (1 0 5), A (2 1 1) and A (1 1 2) at 30.9°, 36.8°, 42.2°, 48.1°, 54.4°, 55.1° and 66.1° respectively, crystallite sizes determined using the Scherer formula for most instance three peaks at 25.3°, 30.9° and 36.8° are 3.8, 5.7 and 7.1 nm respectively. Strongest peak for TiO_2 Nanoparticles synthesized by $TiCl_3$ is observed for A (1 0 1) reflection at $2\Theta = 25.3°$. Other crystalline plans comes at B (1 2 1), A (0 0 4), A (2 0 0), A (1 0 5), A (2 1 1) and A (1 1 2) at 30.9°, 36.8°, 48.1°, 54.4°, 55.1° and 66.1° respectively, crystallite sizes determined using the Scherrer formula for most instance three peaks at 25.3°, 30.9° and 36.8° are 14.8, 15.2 and 16.0 nm respectively. Absence of other/unidentified reflection peak in XRD analysis shows that no other phase/impurity is present in samples.

Peak area analysis, fitted by Gaussian curves method of XRD pattern and its comparison with JCPDS files (No. 21-1272) and (No. 29-1360) shows that $TiCl_4$ give brookite (61.23%) crystalline phase dominantly while $TiCl_3$ gives anatase (92.58%) phase predominantly. The dominance of brookite phase for TiO_2 nanoparticles, synthesized by $TiCl_4$ at low temperature hydrolysis may be due to its

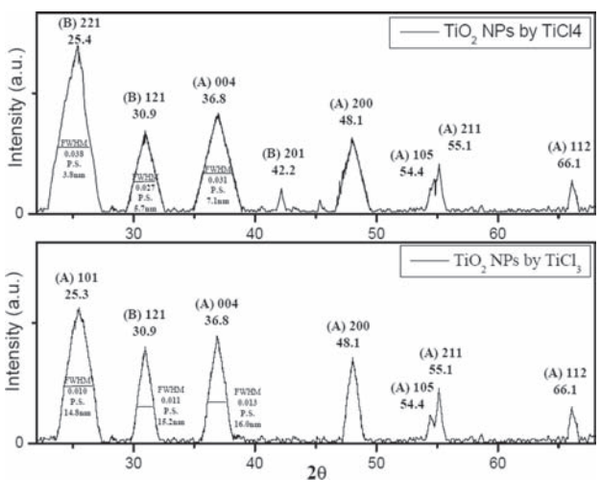

Figure 1. X-ray diffraction pattern of TiO_2 Nanoparticles synthesized by $TiCl_4$ and $TiCl_3$ respectively. Crystallite sizes, crystalline phase and corresponding reflection at 2Θ is also marked at top of peaks, with reference to diffraction data from JCPDS files for anatase (No. 21-1272) and brookite (No. 29-1360), where A denotes anatase and B denotes brookite crystalline phase. FWHM (full writhe at half maximum, in radians) obtained from Peak area analysis fitted by Gaussian curves method and P.S. (particle size) calculated using Scherrer formula for most instance three peaks are also marked in middle of peak. Average particle comes out to be 6 and 16 nm for particles synthesized by $TiCl_4$ and $TiCl_3$ respectively.

very small particle size and narrow particle size distribution or it may be due to presence of Chloride ions in solution to form stable complexes with Ti (IV) as explained by Pottier.[34] Other factors which may control size and phase of the particles is temperature, PH and concentration of precursors. As Addamo and coworkers observed that at low temperature synthesis, presence of brookite, anatase and rutile phases were very sensitive to the volume ratio of $TiCl_4$ to water, i.e., at 1:50 $TiCl_4$ to water ratio rutile and brookite are dominant phases, whereas in the case of a 1:100 ratio dominant phase was anatase.[35] Solution composition is also responsible for phase present as evident from the fact that in sulphate containing media, the dominant phase is rutile.[36, 37]

TEM image of TiO_2 nanoparticles is obtained same day after stirring of 24 hrs completed. The TiO_2 nanoparticles are vacuum dried and re-dispersed in acetone by ultra-sonication, to ensure that there is no HCl present in the samples. Figure 2(a) shows TEM image of TiO_2 nanoparticles synthesized by $TiCl_4$ with particle size ranging from 6–10 nm and Figure 2(c) shows TEM image of TiO_2 nanoparticles synthesized by $TiCl_3$ with particle size ranging from 15–20 nm. Figures 2(b) and (d) also shows electron diffraction pattern of these TiO_2 nanoparticles. Patterns are analyzed and marked in terms of lattice planes and results are one to one matching with crystalline planes of XRD, indicating that the particles are crystalline. No significant aggregation of particles are visible in the TEM image.

Important feature of XRD and TEM analysis is that average particle size determined by XRD were 6 and 15 nm for TiO_2 nanoparticles synthesized by $TiCl_4$ and $TiCl_3$ respectively (Fig. 1), which is smaller than the size range obtained by TEM images in both the cases. Here XRD analysis was done after five days of synthesis while TEM measurement was done immediately after completion of synthesis, indicates that there is no aggregation in TiO_2 nanoparticles having surface free from organic capping agent even with time.

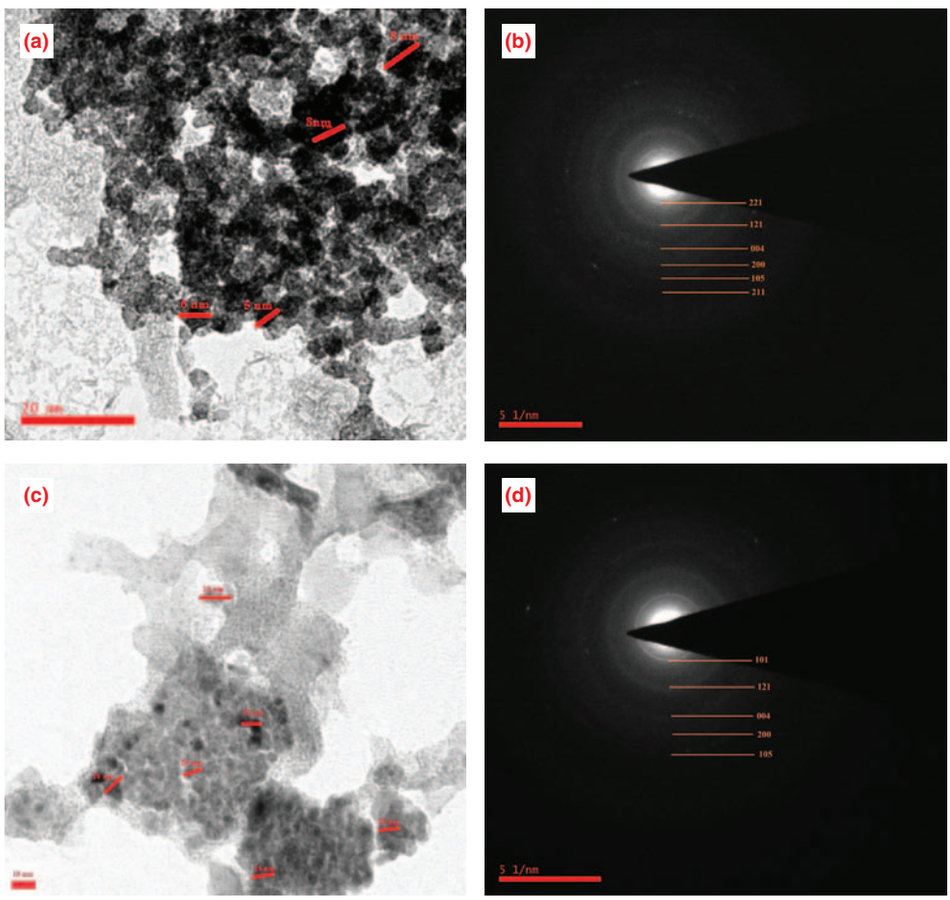

Figure 2. Transmission electron micrographs (TEM) of TiO_2 nanoparticles synthesized by two different precursors of Ti i.e., $TiCl_4$ and $TiCl_3$ are (a), (c) respectively. Both images are marked with red arrow showing particle diameter, marking was done for smallest, intermediates and largest particle of image so that range for Crystallite sizes can be calculated, it comes out 5–10 nm and 15–20 nm for particles synthesized by $TiCl_4$ and $TiCl_3$ respectively. Whereas (b), (d) are showing electron diffraction pattern for particles synthesized by $TiCl_4$ and $TiCl_3$ respectively, marked with crystalline planes that indicates particles as being crystalline.

In present scenario, TEM images and XRD pattern is best indicator of particle size, phase and purity of the samples, but to determine aggregation present in sample and presence of any type of impurity in samples, especially Cl content that causes fast aggregation in particle, SEM and EDAX measurements are recorded to verify morphology and chemical analysis.[38] To avoid gold coating on samples, samples were prepared on conducting Si substrate. After ten days of completion of synthesis, few drops (that is more them ten times higher in amount at per unit area, comparatively to the sample used for TEM analysis) directly from stable particle dispersion stored at 0 °C of TiO_2 nanoparticles loaded on different Si substrate and allowed to dry at room temperature in a closed chamber then analyzed by SEM. Figures 3(a) and (c) show SEM image and EDAX analysis of TiO_2 nanoparticles synthesized by $TiCl_4$ having particle size ranging from 8–11 nm. While Figures 3(b), (d) also shows SEM image and EDAX analysis of TiO_2 Nanoparticles synthesized by $TiCl_3$ having particle size ranging from 18–22 nm. Here in both cases the crystallite size is almost similar to as observed from TEM and XRD, i.e., it is clear that nanoparticles seen by SEM image consist same number of crystallites which is seen by TEM image i.e., there is no agglomeration present in the samples even after ten days of synthesis and even with higher amount/concentration of TiO_2 nanoparticles in samples. EDAX analysis is performed on Si substrate, hence it shows highest peak for Si, but no peaks other than Ti, O and Si is present, confirm purity of nanoparticles synthesized. No signal for Cl confirms its complete vaporization during synthesis in form of HCl. Weight% of elements is also tabularized with EDAX analysis image.

Different sizes and shapes makes significant effect on optical properties of nanomaterial. Which is markedly different form corresponding bulk material. Here optical properties are determined by UV-Vis and PL spectroscopy. The UV-visible absorption spectra of TiO_2 nanoparticles samples taken immediately after synthesis are shown in Figure 4(a), while absorption spectra obtained using tauc relation $\{\alpha h\nu = K(h\nu - E_g)^n\}$ to determine band gap of synthesized nano particle is shown in Figure 4(b), Where $h\upsilon$ is the photon energy, α is the absorption coefficient, K is a constant relative to material, E_g is the band gap of material and n depends on nature of transitions, n may have values 1/2, 2, 3/2 and 3 correspond to allowed direct, allowed indirect, forbidden direct and forbidden indirect transitions respectively. Here $n = 1/2$ for direct allowed transition is used.[39,40] The optical energy band gap (E_g) for nanoparticles can be calculate by extrapolating $(\alpha h\nu)^2$ versus $h\nu$ at zero absorption coefficient.

UV-Vis absorption band edges were observed at 3.81 eV for TiO_2 nanoparticles synthesized by $TiCl_4$ and 3.68 eV TiO_2 nanoparticles synthesized by $TiCl_3$. The surface plasmon resonance for samples were calculated using relation $\lambda = hc/E_g$, which comes around 325 nm and 337 nm respectively in ultraviolet region. Larger value of band gap E_g/(SPR) of prepared TiO_2 nanoparticles compare to bulk value 3.2 eV/(409 nm), can be explained on basis of band gap dependence on particle size. The band gap increases

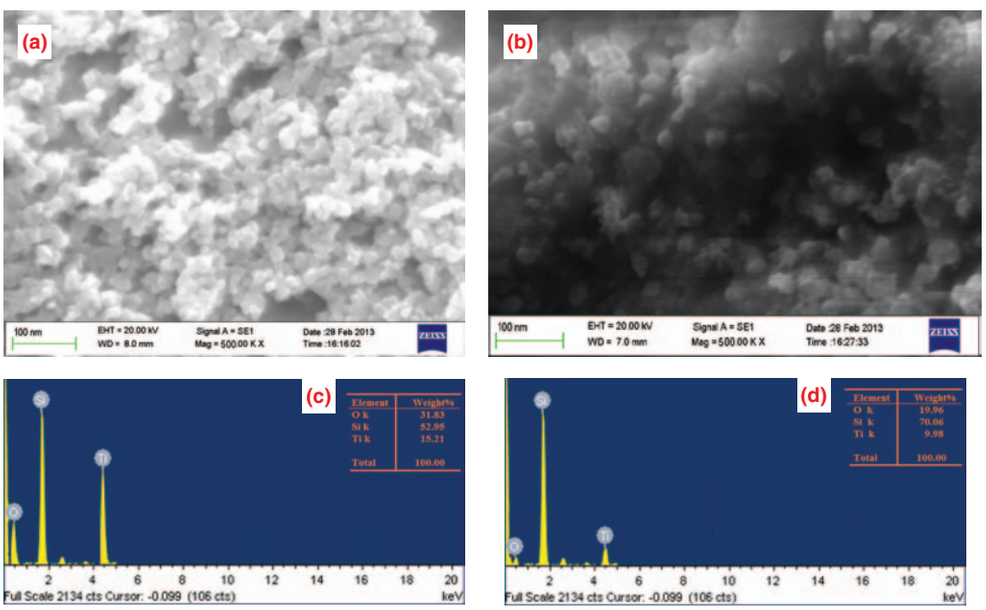

Figure 3. Scanning electron micrographs (SEM) of TiO_2 nanoparticles synthesized by two different precursors of Ti i.e., $TiCl_4$ and $TiCl_3$ are (a) and (b) respectively, not showing any aggregation in particles. Whereas (c) and (d)are EDAX analysis for particles synthesized by $TiCl_4$ and $TiCl_3$ respectively, only peaks for Ti, O and Si is present (measurements were performed on conducting Si Substrate), even no signal for Cl is present, shows purity of synthesized nanoparticles. Weight% of these elements were also tabularized with EDAX analysis image.

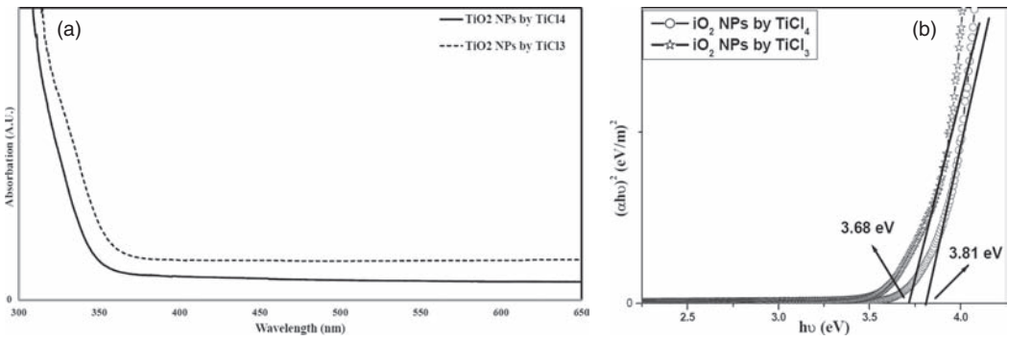

Figure 4. UV-Vis absorption spectrum and spectrum obtained using tauc relation for TiO_2 nanoparticles synthesized by $TiCl_4$ and $TiCl_3$. UV-Vis band gap (absorption band edges) were observed at 3.81 eV (325 nm) and 3.68 eV (337 nm) for TiO_2 nanoparticles synthesized by $TiCl_4$ and $TiCl_3$ respectively are much higher (smaller) than these values 3.2 ev/(409 nm) of bulk TiO_2.

with decreasing particle size and this gives blue shift in absorption edge. Considering blue shift of SPR relative to bulk TiO_2, absorption onset can be assigned to direct transition type of electrons in TiO_2 nanoparticles. Here also results are agree for the particle size as obtained from TEM/SEM/XRD. TiO_2 nanoparticles synthesized by $TiCl_4$ giving smaller size nanoparticles (5–10 nm) having higher band gap 3.81 eV, compared to synthesized by $TiCl_3$ having particle size (15–20 nm) and band gap 3.68 eV, showing relative blue shift of 12 nm corresponding to energy difference of 0.13 eV.

Photoluminescence (PL) emission spectra of nanoparticles synthesized using different precursors of Ti are shown in Figure 5, taken immediately after synthesis of nanoparticles. PL emission spectra are recorded at selected excitation wavelength of 331 nm, which is average value of maximum absorption/SPR for nanoparticles synthesized by $TiCl_4$ (SPR = 325 nm) and $TiCl_3$ (SPR = 337 nm). A broad PL emission band occur ranging 348–562 nm centered at λ_{max} 392 nm, calculated band gap value for this wavelength is 3.160 eV for TiO_2 nanoparticles synthesized by $TiCl_4$, while TiO_2 nanoparticles synthesized by $TiCl_3$ gives broad PL emission band ranging 364–576 nm centered at λ_{max} 410 nm, calculated band gap value for this wavelength is 3.025 eV, corresponds to direct recombination between electrons in conduction band and holes in the valence band. The difference in band gap for both samples comes out to be 0.135 eV (3.160–3.025) is in close agreement with absorption band gap difference 0.13 eV (3.81–3.68) obtained from UV-Vis spectroscopy, while both the samples are excited with same energy/wavelength. A striking feature of this analysis comes that PL emission edges ($\lambda_{max} = 410$ nm, $E_{max} = 3.025$ eV and $\lambda_{max} = 392$ nm, $E_{max} = 3.160$ eV) of these synthesized Nanoparticles are similar or smaller than the absorption value ($\lambda_g = 410$ nm, $E_g = 3.025$ eV) of bulk TiO_2, hence by mixing these Nanoparticles with bulk TiO_2, it could be possible to design optical filters (to absorb a particular band) such that emission edge of one (nanoparticles) can be absorbed by the absorption edge of bulk/other material.

The effect of TiO_2 nanoparticles on survival of *E. coli* bacteria under fluorescent light is shown in Figure 6.

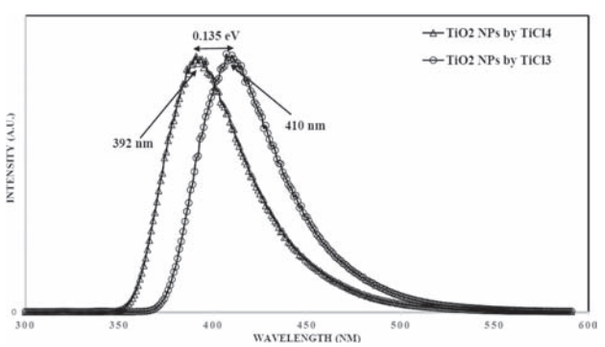

Figure 5. Photoluminescence (PL) emission spectra of TiO_2 nanoparticles synthesized by $TiCl_4$ and $TiCl_3$, recorded at excitation wavelength of 331 nm (which is average value of maximum UV absorption/SPR for both nanoparticles synthesized by $TiCl_4$ (325 nm)). and $TiCl_3$ (337 nm). The difference in band gap 0.135 eV (3.160–3.025) is in closely agree with absorption band gap difference 0.13 eV (3.81–3.68) obtained from UV-Vis spectroscopy.

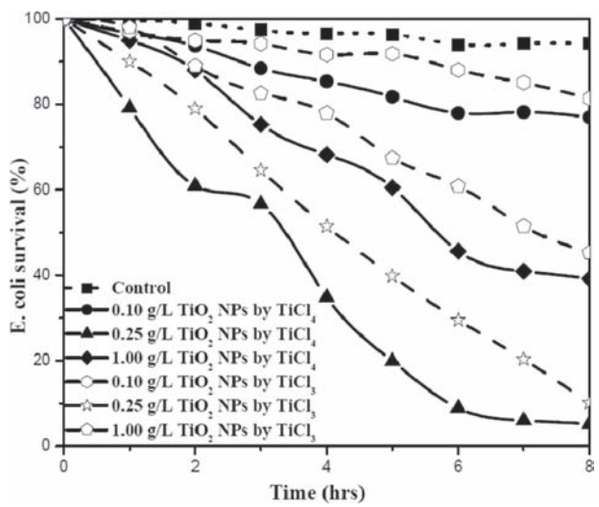

Figure 6. The effect of TiO_2 nanoparticles synthesized by using different precursors of Ti, on survival of *E. coli* during photo-catalytic process.

Survival percentage of *E. coli* is decreases with illumination time for three different TiO_2 concentrations. If there is absence of TiO_2 in sample then only ≈6% of bacteria are inactivated. Optimum inactivation was achieved at 0.25 g/L concentration of TiO_2 nanoparticles synthesized by $TiCl_4$ where ≈94% of *E. coli* was inactivated in 8 hrs., while for 0.1 g/L of TiO_2 concentrations only ≈20% *E. coli* were inactivated in 8 hrs. i.e., it is insufficient for inactivation of *E. coli*, meanwhile at 1.0 g/L of TiO_2 concentration ≈60% *E. coli* were inactivated in 8 hrs., it may be due to saturation in suspension that cause absorption, scattering and shadowing effect of UV light by the top most particles in the medium, thus reduced extent of UV light can reach all the particles in suspension as suggested by Coleman et al.[41]

Same concentration dependent effect was observed for TiO_2 nanoparticles synthesized by $TiCl_3$, where ≈16%, ≈89% and ≈55% *E. coli* bacteria were inactivated by the 0.1, 0.25 and 1.0 g/L concentrations of TiO_2 under UV light respectively, that is less than *E. coli* inactivated by TiO_2 synthesized by $TiCl_4$. Because for larger particles (synthesized by $TiCl_3$) scattering and shadowing effect of UV light by the top most particles will increased in the medium, which reduces extent of UV light that can reach to all particles in suspension, hence less number of *E. coli* were inactivated in suspension having larger size particles.

If fluorescent illumination will continues for a sufficient time, *E. coli* will be completely mineralized and produce CO_2, H_2O and other mineral compounds.[42] This mechanism of photo-catalysis of TiO_2 on *E. coli* illumination was enplaned by Sunada et al.[43] into three stages:

(1) Outer membrane of *E. coli* was attacked and partially decomposed by reactive species such as $^{\bullet}OH$, O_2^- and H_2O_2.

(2) Disordering of inner membrane leading to peroxidation of lipid membrane thus killing the cell.

(3) Decomposition of the dead cell.

4. CONCLUSION

In present study we have synthesized titanium dioxide (TiO_2) nanoparticles using two different precursor of Ti i.e., $TiCl_4$ and $TiCl_3$ by aqueous hydrolysis and basic oxidization respectively having clean surfaces free from organic compounds and capping agents, to be used in future interfacial studies. The average size less than 20 nm of TiO_2 is confirmed by TEM, SEM and XRD. This analysis confirm no agglomeration in particles even synthesized without using any capping/stabilizing agents or even at higher concentration. Crystalline planes obtained from X-ray diffraction are well agree with electron diffraction pattern of TEM. XRD phase analysis also shows dominant brookite crystalline phase occur for TiO_2 nanoparticles synthesized by $TiCl_4$, while anatase crystalline phase predominant for TiO_2 nanoparticles synthesized by $TiCl_3$. EDAX analysis proves purity of synthesized nanoparticles, even no signal peak for Cl was detected. Optical properties showing increase in band gap with decrease in particle size. UV-Vis absorption band edges (SPR) were observed at 3.81 eV (325 nm) and 3.68 eV (337 nm) for TiO_2 nanoparticles synthesized by $TiCl_4$ and $TiCl_3$ respectively, while PL emission peak were observed at 392 nm and 410 nm respectively for excitation at 331 nm, are closely matching. A striking feature of this analysis comes that PL emission edges ($\lambda_{max} = 410$ nm, $E_{max} = 3.025$ eV and $\lambda_{max} = 392$ nm, $E_{max} = 3.160$ eV) of these synthesized nanoparticles are similar or smaller than UV absorption value ($\lambda_g = 410$ nm, $E_g = 3.025$ eV) of bulk TiO_2. TiO_2 nanoparticles synthesized are viable material for inactivation of *E. coli* by photo-catalysis. 0.1 g/L is not enough and at 1.0 g/L is too high concentrations of TiO_2 nanoparticles and can't give effective inactivation of *E. coli*. However, TiO_2 nanoparticles concentration at 0.25 g/L is sufficient to inactivated 115 cfu/mL of *E. coli* under fluorescent light. This phenomena is also size dependent and as the particle size increase the efficiency of inactivation of *E. coli* get reduced.

Acknowledgment: Authors are thankful to Mr. Raza and Mr. Sachin Surve of USIC for helping in TEM and SEM measurements. Authors are also thankful for Department of Physics, University of Rajasthan for providing facilities for XRD measurements and USIC, University of Rajasthan for providing facilities for TEM and SEM analysis.

References and Notes

1. A. Fujishima and K. Honda, *Nature* 238, 37 **(1972)**.
2. A. Fujishima, X. T. Zhang, and D. A. Tryk, *Sur. Sci. Reports* 63, 515 **(2008)**.
3. M. K. Nowotny, L. R. Sheppard, and T. B. Nowotny, *J. Phys. Chem. C* 112, 5275 **(2008)**.
4. N. Serpone, D. Lawless, and R. Khairutdinov, *J. Phys. Chem.* 99, 16646 **(1995)**.
5. L. Gao and Q. H. Zhang, *Scripta Mater.* 44, 1195 **(2001)**.
6. H. Nakabayashi, N. Kakuta, and A. Ueno, *Bull. Chem. Soc. Japan* 64, 2428 **(1991)**.
7. V. H. Grassian, *J. Phys. Chem. C* 112, 18303 **(2008)**.
8. L. X. Chen, T. Rajh, Z. Y. Wang, and M. C. Thurnauer, *J. Phys. Chem. B* 101, 10688 **(1997)**.
9. O. Carp, C. L. Huisman, and A. Reller, *Prog. Solid State Chem.* 32, 133 **(2004)**.
10. P. Agarwal, R. Agarwal, and N. K. Agrawal, 58th DAE-Solid State Physics Symposium, AIP Proceedings, Patiala, December **(2013)**.
11. P. Pimpliskar, B. Bagra, A. Sharma, S. Khandwal, and N. K. Agrawal, 58th DAE-Solid State Physics Symposium, AIP Proceedings, Patiala, December **(2013)**.
12. M. R. Mohammadia, D. J. Fray, and M. C. Cordero-Cabrera, *Sensors Actuators. B* 124, 74 **(2007)**.
13. Y. Q. Wang, H. M. Zhang, and R. H. Wang, *Col. Surf. B: Biointerfaces* 65, 190 **(2008)**.
14. M. Sairam, M. B. Patil, R. S. Veerapur, S. A. Patil, and T. M. Aminabhavi, *J. Mem. Sci.* 281, 95 **(2006)**.
15. A. Wood, M. Giersig, and P. Mulvaney, *J. Phys. Chem. B* 105, 8810 **(2001)**.
16. B. Regan and M Gratzel, *Nature* 353, 737 **(1991)**.
17. H. Tada, T. Ishida, and A. Takao, *Langmuir* 20, 7898 **(2004)**.

18. P. Agarwal, A. Mehta, S. Kachhwaha, and S. L. Kothari, *Adv. Sci. Eng. Med.* 5, 709 **(2013)**.

19. R. Agarwal, N. K. Agrawal, and R. Singh, *Adv. Sci. Eng. Med.* 6, 203 **(2014)**.

20. N. K. Agrawal, N. A. Kumar, M. Singh, Y. K. Vijay, and K. C. Swami, 58th DAE- Solid State Physics Symposium, AIP Proceedings, Patiala, December **(2013)**.

21. R. Chu, J. Yan, S. Lian, Y. Wang, F. Yan, and D. Chen, *Solid State Commun.* 130, 789 **(2004)**.

22. K. Kanie and T. Sugimoto, *Chem. Commun.* 82, 1584 **(2004)**.

23. C. Lao, L. Y. Chuai, L. Su, X. Liu, L. Huang, H. Cheng, and D. Zou, *Solar Energy Mater. Solar Cells* 85, 457 **(2005)**.

24. D. W. Bahnemann, *Israel J. Chem.* 33, 115 **(1993)**.

25. J. H. Lee and Y. S. Yang, *J. Eur. Ceramic Soc.* 25, 3573 **(2005)**.

26. J. I. Langford and A. J. C. Wilson, *J. Appl. Crystallography* 11, 102 **(1978)**.

27. R. C. Nadia, F. Machado, and V. S. Santana, *Catalysis Today* 108, 595 **(2005)**.

28. N. K. Agrawal, K. Awasthi, Y. K. Vijay, and K. C. Swami, *J. Adv. Electrochem.* 2, 31 **(2013)**.

29. K. P. Kuhn, I. F. Chaberny, K. Massholder, M. Sticker, V. W. Benz, H. G. Sonntag, and L. Erdinger, *Chemosphere* 53, 71 **(2003)**.

30. P. Thevenot, J. Cho, D. Wavhal, R. B. Timmons, and L. Tang, *Nanomed. Nanotech. Bio. Med.* 4, 226 **(2008)**.

31. L. Zan, W. J. Fa, T. Y. Peng, and Z. K. Gong, *J. Photochem. Photobiol. B* 86, 165 **(2007)**.

32. A. K. Benabbou, Z. Derriche, C. Felix, P. Lejeune, and C. Guillard, *Appl. Catalyst B* 76, 257 **(2007)**.

33. A. Hamzah, A. Rabu, R. F. Hanim, R. Azmy, and N. A. Yussoff, *Sains Malaysiana* 39, 161 **(2010)**.

34. A. Pottier, C. Chaneac, E. Tronc, L. Mazerolles, and J. P. Jolivet, *J. Mater. Chem.* 11, 1116 **(2011)**.

35. M. Addamo, V. Augugliaro, A. D. Paola, E. Garcia-Lopez, V. Loddo, G. Marci, and L. Palmisano, *Coll. Surf. A–Phys. Eng. Aspects* 265, 23 **(2005)**.

36. Q. H. Zhang, L. Gao, and J. K. Guo, *J. Nanostructured Mater.* 11, 1293 **(1999)**.

37. B. Bagra, P. Pimpliskar, and N. K. Agrawal, 58th DAE-Solid State Physics Symposium, AIP Proceedings, Patiala, December **(2013)**.

38. N. K. Agrawal, Y. K. Vijay, and K. C. Swami, *J. Mater. Sci. Surf. Eng.* 1, 19 **(2014)**.

39. A. M. Salem and M. S. Selim, *J. Phys. D Appl. Phys.* 34, 12 **(2001)**.

40. R. Maity and K. K. Chattopadhyay, *Nanotechnology* 15, 812 **(2004)**.

41. H. M. Coleman, C. P. Marquis, J. A. Scott, S. S. Chin, and R. Amal, *Chem. Eng. J.* 113, 55 **(2005)**.

42. A. Fujishima, T. N. Rao, and D. A. Tryk, *J. Photochem. Photobiol. C* 1, 1 **(2000)**.

43. K. Sunada, T. Watanabe, and K. Hashimoto, *J. Photochem. Photobiol. A* 156, 227 **(2003)**.

Received: 22 August 2013. Accepted: 20 November 2013.